Evaluation of the potential therapeutic effects of a double-stranded RNA mimic complexed with polycations in an experimental mouse model of endometriosis

Carmen Maria García-Pascual, Ph.D.,[a,b] Jessica Martínez, Ph.D.,[a] Paula Calvo, M.D.,[c] Hortensia Ferrero, Ph.D.,[a,b] Ana Villanueva, Ph.D.,[d] Mercedes Pozuelo-Rubio, Ph.D.,[d] Marisol Soengas, Ph.D.,[e] Damiá Tormo, Ph.D.,[d] Carlos Simón, M.D.,[a,b] Antonio Pellicer, M.D.,[b,c] and Raúl Gómez, Ph.D.[a]

[a] Instituto Universitario IVI/INCLIVA, Valencia; [b] Fundación IVI, Parque Científico Universidad de Valencia, Paterna; [c] Departamento de Ginecología, Hospital Universitario y Politécnico La Fe, Valencia; [d] Bioncotech Therapeutics, Paterna; and [e] Melanoma Laboratory, Molecular Pathology Programme, Centro Nacional de Investigaciones Oncológicas (Spanish National Cancer Research Centre), Madrid, Spain

Objective: To assess the therapeutic potential of polyinosine-polycytidylic acid, a double-stranded RNA molecule with selective proapoptotic and antiangiogenic activity, complexed with polyethyleneimine (pIC^{PEI}) in treating endometriosis.
Design: A heterologous mouse model of endometriosis was created by injecting human endometrial fragments into the peritoneum. Endometrial fragments were engineered to express the fluorescent protein mCherry as a reporter to monitor status over the course of the 4-week study.
Setting: University-affiliated infertility center.
Animal(s): Ovariectomized and hormone-replaced nude mice (n = 30) injected with fluorescent-labeled human endometrial fragments at 4–6 weeks of age.
Intervention(s): Animals (n = 10 per group) were injected with vehicle (control), the anti-VEGF compound CBO-P11 (0.6 mg/kg), or pIC^{PEI} (0.6 mg/kg) twice weekly over the course of 4 weeks.
Main Outcome Measure(s): Variations in the size of endometriotic implants were estimated by quantifying the expression of mCherry throughout the course of the experiment. Neovascularization, cellular proliferation, and apoptosis were estimated by quantitative immunofluorescence detection of PECAM, α-SMA, Ki67, and TUNEL.
Result(s): pIC^{PEI} promoted a significant increase in apoptosis and a decrease in neovascularization in human fragments, but did not reduce the size of endometriotic implants.

Received June 19, 2015; revised July 17, 2015; accepted July 22, 2015; published online August 18, 2015.
C.M.G.-P. has nothing to disclose. J.M. has nothing to disclose. P.C. has nothing to disclose. H.F. has nothing to disclose. A.V. has nothing to disclose. M.P.-R. has nothing to disclose. M.S. holds patent WO 2011003883 A1 for the treatment of tumors with the use of pIC^{PEI}. D.T. has stock options in Bioncotech, the company providing the pIC^{PEI} compound tested in this study, and holds patent WO 2011003883 A1 for the treatment of tumors with the use of pIC^{PEI}. C.S. has nothing to disclose. A.P. has nothing to disclose. R.G. has nothing to disclose.
Supported by the Spanish Ministry of Economy and Competitiveness through a Miguel Servet Program (CP13/00077) cofunded by FEDER (European Regional Development Fund) and ISCIII (Carlos III Institute of Health) grants (PI14/00547) awarded to R.G. and by the Valencia State Government through a Prometeo grant (20100613) awarded to A.P.
C.M.G.-P's. current affiliation: Division of Obstetrics and Gynecology, Department of Women's and Children's Health, Karolinska Institutet, Karolinska University Hospital, Stockholm, Sweden, as a fellow from the Marie Curie Program.
Reprint requests: Raúl Gómez, Ph.D., Instituto Universitario/INCLIVA, Avda. Menéndez Pelayo 4 Accesorio, 46010-Valencia, Spain (E-mail: raulgomgal@gmail.com).

Fertility and Sterility® Vol. 104, No. 5, November 2015 0015-0282/$36.00

http://dx.doi.org/10.1016/j.fertnstert.2015.07.1147

Conclusion(s): While pIC^{PEI} treatment had significant antiangiogenic and pro-apoptotic effects in this setting, longer periods of exposure than the ones supported by our heterologous model and/or assays in homologous mouse models of endometriosis may be necessary to detect an effect of this compound on lesion size. (Fertil Steril® 2015;104:1310–8. ©2015 by American Society for Reproductive Medicine.)
Key Words: Endometriosis, angiogenesis, apoptosis, mouse model, pIC^{PEI}

Endometriosis is an estrogen-dependent gynecologic disease, pathologically defined by the presence of endometrial tissue, glands, and stroma outside of the uterine cavity (1). It occurs when tissue shed from the uterine lining through retrograde menstruation implants and grows outside of the uterus (2). More than 15% of women of reproductive age are estimated to have endometriosis, with one-half of them presenting with the classic symptoms of pelvic pain and infertility (3, 4). Although surgery provides temporary relief, recurrence can occur in up to 75% of cases within 2 years (3). Conventional pharmacologic treatments often fail to provide long-term relief and cause a hypoestrogenic state linked to secondary effects (i.e., bone mineral density loss, suffocation, and palpitations related to a pseudomenopausal state) (5).

An adequate blood supply is essential to ectopic endometrial growth (6, 7). Therefore, inhibition of angiogenesis with commercial antiangiogenic oncologic drugs has been successfully used to treat endometriosis in mouse models (8). However, owing to their toxic nature, the use of these drugs is not feasible in otherwise healthy women (9, 10). One way to circumvent this limitation would be to use antiangiogenic drugs with a lesser toxic profile (11, 12).

Polyinosine-polycytidylic acid (pIC) is a double-stranded synthetic RNA (dsRNA) mimic (13) described more than 4 decades ago to exert antitumoral activities in immunocompetent rodents by means of immunomodulation of the interferon pathway (14). Very early, however, Fisher et al. revealed (15) that pIC-induced regression of tumor growth might also be achieved in irradiated mice. This finding suggested that antitumoral activity of pIC might be exerted by means of additional nonimmunostimulatory effects. In this regard later studies revealed that suppression of angiogenesis by the stimulation of the Toll-like receptor 3 might account for the therapeutic effects of pIC in immunocompromised tumor animal models (16, 17). The favorable toxic profile (18) and the mentioned powerful antitumoral activity in animal models (14) encouraged clinical early trials, in which naked pIC showed, however, no detectable antitumor effects (19, 20). Nevertheless, clinical trials using pIC for the treatment of malignant cancers have been recently launched again with promising results (21, 22) since the discovery that vehicle delivery, in the form of liposomes or polycations, was critical to favor endosomal uptake and cytosolic release of pIC in vivo, (23). In line with this, a study by Tormo et al. (24) in a mouse model of melanoma revealed that by complexing pIC with a carrier, such as polyethyleneimine (PEI), the complex pIC^{PEI} induced selective apoptosis in malignant cells by promoting hyperactivation of autophagy in them. Owing to the fact that no tumor death was observed when naked instead of complexed pIC was administered, it became evident that the carrier, PEI, shifted the mode of action of pIC from innocuous to a persistent transcriptional program with antitumor activity (25).

Because of the similarities in terms of increased angiogenesis and inhibited apoptosis between cancer and endometriosis (26), we empirically hypothesized that pIC^{PEI} might offer a therapeutic tool to treat the latter. To test this, the potential antiangiogenic and proapoptotic activities effects of pIC^{PEI} were quantified and its effects on lesion size were noninvasively assessed in human endometrial fragments implanted into nude mice.

MATERIALS AND METHODS

Generation of mCherry-expressing Vector

Adenoviral stock encoding the fluorescent protein mCherry (Ad-mCherry, 1767) was purchased from Vector Biolabs. Recombinant adenoviruses were amplified with the use of HEK293 FT cells (R7000-7; Invitrogen) to obtain high-titer stock. Adenovirus was purified and titered with the use of a Virabind Adenovirus Purification Kit (VPK-100; Cell Biolabs) and Quicktiter ELISA kit (VPK-110; Cell Biolabs) according to the manufacturer's instructions. Purified viruses were stored at −80°C until use.

Endometrial Tissue Collection

Use of human tissue specimens was approved by the Institutional Review Board and Ethics Committee of the Hospital Universitario La Fe. All patients provided written informed consent. Biopsies of eutopic endometrial tissues (n = 4) at the edge of the late proliferative/early secretory phase were acquired from egg donors at the time of oocyte retrieval procedure. Fresh tissues from each patient were harvested immediately in maintenance medium (M199 medium; Gibco) containing 10% fetal bovine serum (FBS; PAA), antibiotic-antimycotic solution (Gibco), and 10 mmol/L N-2-hydroxyethylpiperazine-N0-2-ethanesulfonic acid (HEPES) buffer solution (PAA) and transported on ice to the laboratory. Biopsies with a lax appearance and/or high amount of mucus were discarded (n = 2). Fragments from the remaining

biopsies with a healthy appearance (n = 2) were placed on a 10-cm Petri dish, cut into 5–10-mm^3 pieces with a scalpel, and punctured carefully with a 27-G syringe to increase the amount of tissue surface exposed. Next, tissue pieces were placed in 96-well plates (2–3 fragments per well) and washed twice with antibiotic-free M199 medium.

Adenoviral Transfection of Endometrial Fragments

Endometrial fragments were incubated with Ad-mCherry (1×10^8 PFU/mL) diluted in antibiotic-free DMEM F-12 (Life Technologies) and 10% FBS (FBS Gold; PAA) medium overnight (12–18 h) at 37°C, with 5% CO_2 inside an incubator with gentle agitation. Tissue fragments were then rinsed with DMEM F-12 twice, and then replaced with fresh DMEM F-12 medium containing 1% antibiotics (streptomycin and penicillin), fungizone (1 μg/mL) (Gibco), and 10% FBS. Fluorescence was observed in the red channel (568 nm) with the use of an inverted microscope (Eclipse; Nikon) and used to select 40–50 endometrial fragments per each biopsy with optimal signal for subsequent engraftment.

Generation of the Endometriosis Mouse Model

A total of 30 6-week-old athymic nude female mice (Charles River Laboratories International) were used in this study. Mice were housed in specific pathogen–free conditions, at 26°C with a 12-h light–12-h dark cycle, and fed ad libitum. All handling was performed in laminar flow filtered hoods. The study was approved by the Institutional Animal Care Committee at the University of Valencia, and all procedures were performed following the guidelines for the care and use of mammals from the National Institutes of Health. To avoid cycle-dependent variations, animals were ovariectomized, and hormone levels were homogenized by 60-day-release capsules containing 18 mg of 17β-E_2 (Innovative Research of America) placed under the neck skin of ovariectomized mice. One week after surgery, two mCherry-labeled human endometrium fragments (~3–5 mm^3 in size) were fixed in the peritoneum of each animal with the use of an n-butyl-ester cyanoacrylate adhesive (3M Animal Care). To allow homogeneous distribution of human tissue, each biopsy (n = 2) contributed to engraft one fragment per mouse.

Pharmacologic Interventions

One week after implantation, the animals were divided into three groups (n = 10 per group) and given 100-μL tail vein injections of MilliQ water vehicle (negative control group), 0.6 mg/kg anti-VEGF compound CBO-P11 (positive control group), or 0.6 mg/kg pIC^{PEI} (experimental group) every 72 hours over the course of 4 weeks. The pIC^{PEI} dose was chosen based on its effective effects over treatment of melanoma in a mouse model in a previous report (24). Mouse behavior and weight were monitored daily, with no noticeable variation.

In Vivo Fluorescent Imaging

Lesion size during the treatment period was indirectly estimated as a function of the extension and intensity of fluorescence emitted by labeled fragments. Noninvasive observation of fluorescence was performed with the use of an IVIS Spectrum Preclinical In Vivo Imaging System (Perkin-Elmer) and related software coupled to an isoflurane gas anesthesia machine (XG-8 Gas Anesthesia System; Xenogen). Immunofluorescence images were acquired by means of epiluminescence with a peak absorption/emission pair filter set at 587 nm and 610 nm, respectively. The field of view was set at 10 cm until the maximum intensity was obtained, as previously described (27). Fluorescence was monitored beginning the day after the labeled fragments were placed; the process was then repeated twice weekly for 4 weeks.

Quantification of In Vivo Fluorescence Images

Images were displayed as false-color photon-counts superimposed on a grayscale anatomic image with the optical intensity (photon flux) expressed as the average radiant efficiency in photons/s/cm^2 (28). Regions of interest (ROIs) corresponding to lesions were automatically established by the software after manually setting a threshold over the lesion showing minimal intensity. Background fluorescence was subtracted from the ROIs, and data were normalized to the time point at which fluorescence was maximal (usually on day 7 after transplantation).

Recovery and Preprocessing of Lesions

After treatment, the animals were killed with the use of CO_2 inhalation and the peritoneal cavity and lesions were carefully excised. Lesions were embedded in optimal cutting medium and stored at −20°C. Frozen fragments were sliced into 8-μm sections at 50-μm intervals, mounted on Superfrost Gold glass slides (Thermo Fisher Scientific), and fixed in acetone at −20°C for analysis.

Detection of Vascularization Profiles, Cellular Proliferation, and Apoptosis

Fluorescent-labeled antibodies against platelet–endothelial cell adhesion molecule (PECAM; a specific vascularization marker) and α–smooth muscle actin (α-SMA; a marker of the muscular layer contained by mature vessels) were used to detect vascularization and estimate neovascularization: PECAM (BD Pharminge) diluted 1:50 and α-SMA (Sigma-Aldrich) diluted 1:200, following protocols previously described by our group (29, 30). Proliferating cells were detected by means of immunostaining against Ki-67, and apoptotic cells were labeled with the use of an Apoptag Isol Dual Fluorescence Apoptosis Detection Kit (DNase Types I and II; Millipore) as previously described also (29, 30).

Quantification of Immunofluorescence

The two major cross-sections obtained in each implant were considered to be representative of the sample. Four random high-power fields were photographed per cross-section with the use of an image analysis system linked to a Nikon Eclipse E400 microscope. Therefore, a total of 16 images (2 implants × 2 cross sections × 4 high-power fields) per mouse were used

for the determination of each parameter of interest. Quantitative analysis of vascularization (PECAM+), cellular proliferation (Ki67 expression), and apoptosis (terminal deoxynucleotide transferase–mediated dUTP nick-end labeling [TUNEL]) were assessed with the use of specific macros created with Image Pro Plus (Media Cybernetics) as previously described (29, 30). To visualize mature and immature vessels, overlapping images corresponding to the simultaneous detection of PECAM and α-SMA were created with the use of Adobe Photoshop CS3. The percentages of mature (PECAM+/α-SMA+) and immature (PECAM+/α-SMA−) vessels in each field were determined by dividing the number of vessel profiles of each type by the total number of vessels present and multiplying by 100.

Statistical Analysis

Statistical analysis was carried out with the use of the Statistical Package for Social Sciences (IBM). Data were expressed as mean ± SEM. An analysis of variance test followed by Tukey post hoc analysis was used to discern the effects of pIC^{PEI} on sample size. Nonparametric Kruskall–Wallis followed by Mann–Whitney tests were used to compare differences in vascularization, α-SMA expression, proliferation, and apoptosis between groups. Differences were considered to be statistically significant when $P<.05$.

RESULTS

Assessment of Endometriotic Lesions by FLI

The amounts of fluorescence provided by endometrial fragments in all groups were similar at the beginning of the experiment (Fig. 1). Overall intensity increased in all groups, reaching a peak 1 week after implantation. After that, a uniform reduction in the photon signal started in all groups and progressively continued until the end of the experiment. Where a decreasing slope in the VEGF group was more prominent, significant differences from the control group became evident only at the beginning of the 3rd week. At the end of the study period, after 28 days of treatment, 60 ± 5.27%,

FIGURE 1

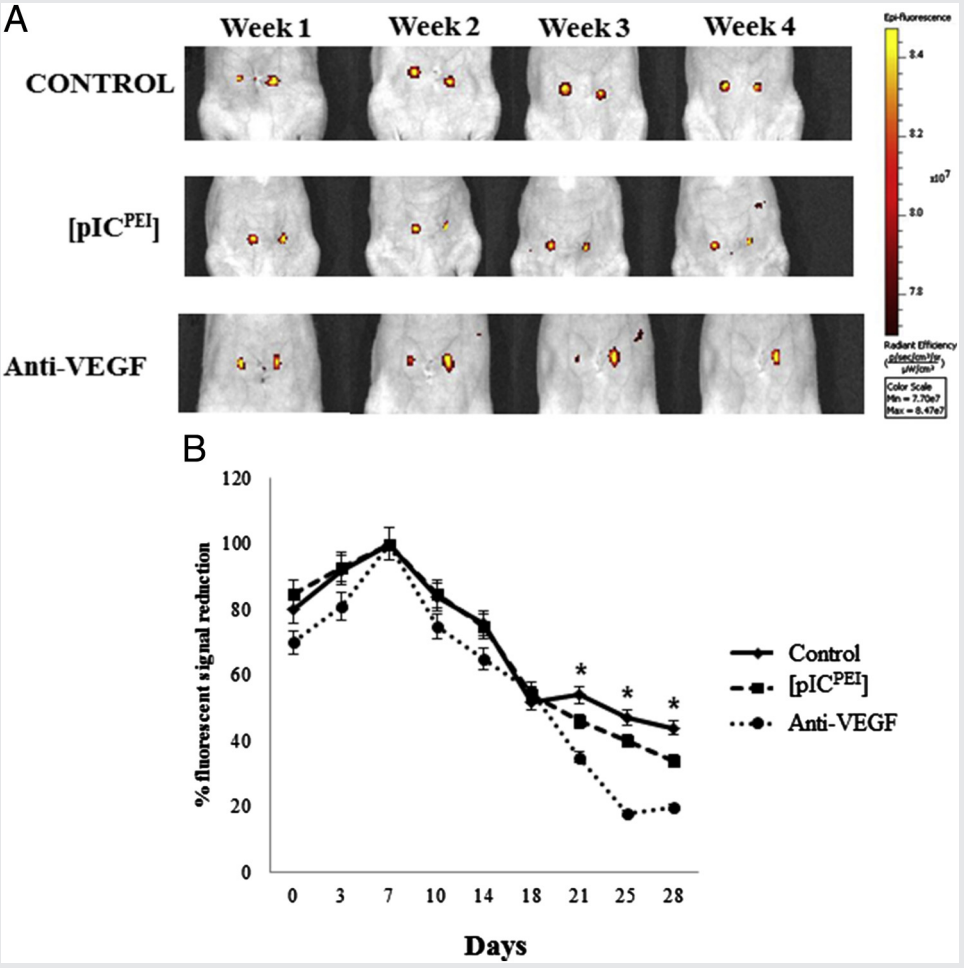

In vivo imaging of endometriotic implants in control, anti-VEGF, and pIC^{PEI} treated animals. (**A**) Examples of the fluorescence signaling provided by mCherry-labeled endometriotic implants in animals monitored during a 4-week time course. (**B**) Quantitative analysis of mean ± SEM fluorescence intensity provided by implants in the three groups during the time course. *$P<.05$ anti-VEGF vs. control group.

García-Pascual. pIC^{PEI} inhibits endometriosis.. Fertil Steril 2015.

65 ± 6.73%, and 80 ± 3.21% decreases in fluorescent signal intensity were quantified for the control, pIC^{PEI}, and anti-VEGF groups, respectively, compared with the point at which signal intensity was maximal at day 7 (Fig. 1). The difference in fluorescent intensity between control and pIC^{PEI}, although noticeable, was not statically significant at the end of the treatment period.

Macroscopic Evaluation of Endometriotic Lesions

In almost all of the animals, both lesions were recovered after treatment. The appearance of implants recovered from the control group was reddish owing to vascularization occurring after implantation. Nearly one-half of the implants of animals treated with anti-VEGF appeared white or pale pink, suggesting a reduction in vascularization. A mix of red, pink, and white implants were observed in pIC^{PEI}-treated animals (Fig. 2).

Quantification of Vascular Density and Maturity in Endometriotic Lesions

Administration of pIC^{PEI} was associated with a noticeable but not statistically significant decrease in vascular density in the lesions compared with negative control (11.90 ± 0.6% vs. 8.76 ± 0.8%), whereas treatment with anti-VEGF antibody (positive control) did cause a significant decrease in this parameter (4.301 ± 0.77%; $P<.05$). We did, however, detect a significant decrease in the number of immature vessels remaining in the pIC^{PEI}-treated animals compared with negative control (Fig. 3).

Cell Proliferation and Apoptosis in Endometriotic Lesions

The percentages of proliferating Ki67 nuclear-stained cells in the endometriotic lesions of animals treated with pIC^{PEI} and anti-VEGF (1.4 ± 0.85% and 1.5 ± 0.9%, respectively) were significantly lower than control (4.3 ± 0.6%; $P<.05$; Fig. 4A). In contrast, the percentages of apoptotic-stained tissue were significantly higher in the endometriotic lesions of animals treated with pIC^{PEI} and anti-VEGF (1.5 ± 0.7% and 1.3 ± 0.9%, respectively) compared with control (0.5 ± 0.4%; $P<.05$; Fig. 4B).

DISCUSSION

Angiogenesis plays a central role in the development of endometriosis, making antiangiogenic therapy a target of therapeutic approaches (7, 8, 31–33). The commercial antiangiogenic drugs currently available are designed for oncologic treatment but are not feasible for treating endometriosis in healthy women owing to high levels of toxicity (9, 34). More specifically, anti–VEGF/VEGFR2 drugs exert nonselective effects over normal vessels, inducing regression of capillaries and thus interfering with processes such as wound healing in which physiologic angiogenesis is required (10). In an effort to overcome these limitations, we and others have sought to investigate the potential for compounds with more selective effects on pathologic vasculature, such as vascular-disrupting agents (11), the dopamine agonist quinagolide (12, 30), and pIC^{PEI}, to treat endometriosis.

FIGURE 2

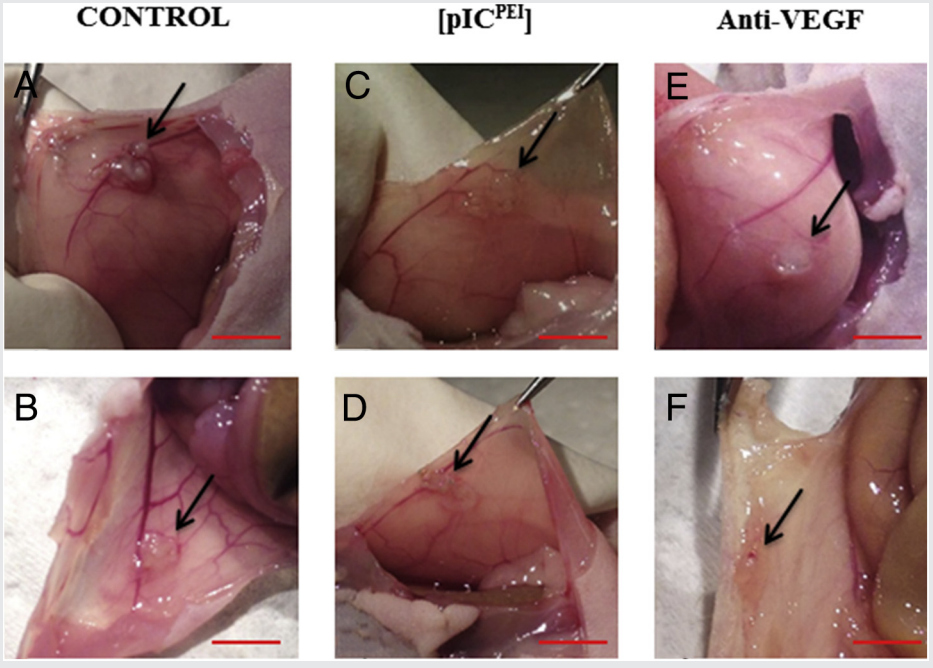

The effect of pIC^{PEI} on macroscopic features of human endometrial implants on the peritoneal wall of mice administered with (**A**, **B**) vehicle, (**C**, **D**) pIC^{PEI}, and (**E**, **F**) the anti-VEGF compound CBO-P11 at the end of the 4-week treatment period. Scale bars = 8 mm.

García-Pascual. pIC^{PEI} inhibits endometriosis.. Fertil Steril 2015.

FIGURE 3

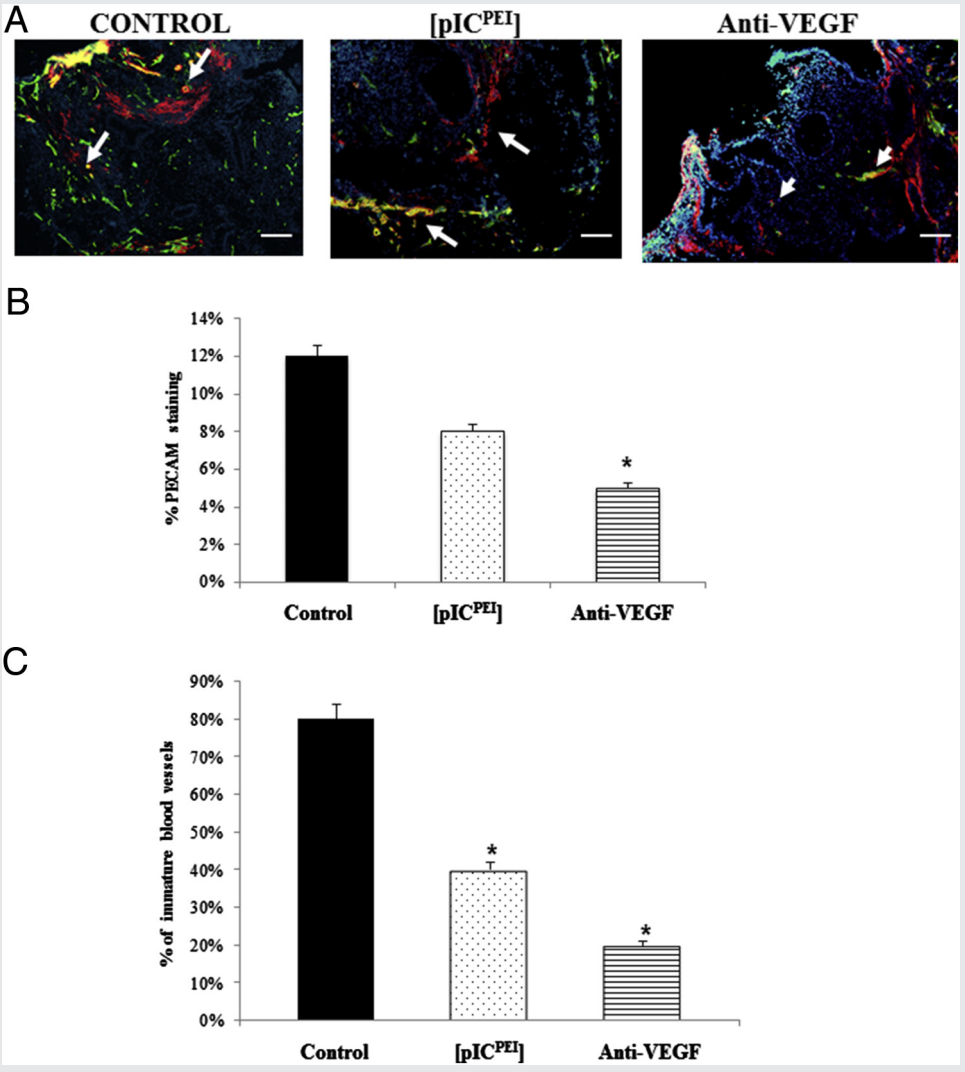

Effect of pIC^{PEI} on vascularization of endometriotic implants. (**A**) Immunofluorescent staining pattern for PECAM (a vascularization marker, staining in *green*) and α-SMA (a muscular layer marker of mature vessels, staining in *red*) in endometriotic implants obtained after killing the mice treated with control, anti-VEGF, or pIC^{PEI}. Mature vessels are identified by overlapping *yellow color*. Scale bar = 150 μm. (**B**) Vascularization as represented by the percentage of PECAM staining (*green*) vs. total area. (**C**) Percentage of immature vessels as represented by the number of immature, not surrounded by a *red muscular layer*, vessels (PECAM+/α-SMA−) divided by the total number of vessels (PECAM+). *P<.05 vs. control group.

García-Pascual. pIC^{PEI} inhibits endometriosis.. Fertil Steril 2015.

Recently, we observed that pIC^{PEI} was able to promote apoptotic activity under more benign conditions of disease, such as leiomyoma (unpublished observations), than the malignant conditions of melanoma in which the proapoptotic activity of this compound was originally described (24). Therefore we inferred that pIC^{PEI} might retain the antiangiogenic properties of poly I:C (16, 17) while simultaneously exerting proapoptotic effects on endometriotic tissue, thus rendering a double therapeutic effect for the treatment of the disease.

To test this hypothesis, we developed a heterologous animal model of endometriosis in which human endometrial fragments were labeled with mCherry (Ad-mCherry) before being implanted into nude mice. We chose to use mCherry instead of green fluorescent protein (GFP) as a reporter for tagging the human tissue because GFP has been shown to result in poor tissue penetration owing to its short emission spectrum, which is not ideal for the visualization of intraperitoneal fragments (35–37). In our model, noninvasive visualization of intraperitoneal implants was possible because mCherry emits a highly photostable, strong, and bright signal with a long wavelength in the red channel (38). The limitation of our and other similar recently developed models (38) is that fluorescence can not be monitored beyond 4–6 weeks owing to the episomal transient expression of the Ad-virus used for labeling

FIGURE 4

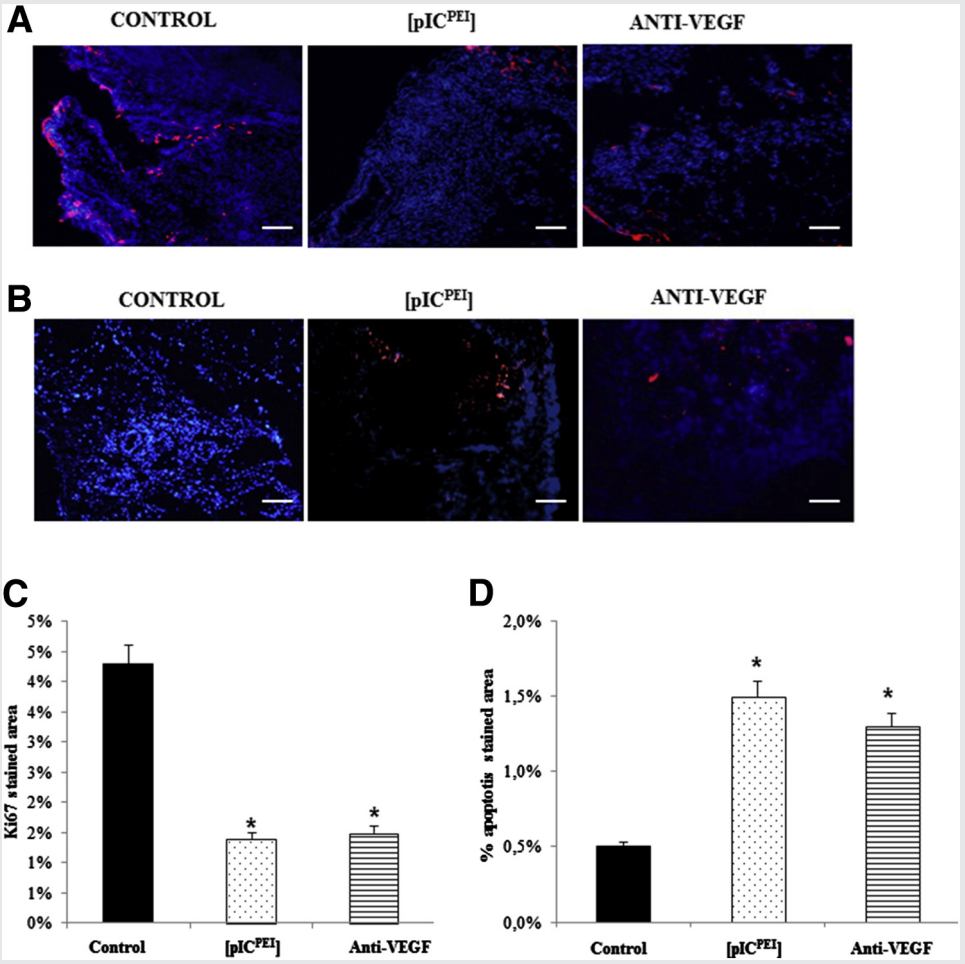

Effect of pIC^{PEI} treatment on cell proliferation and apoptosis of endometriotic implants. (**A**) Proliferating cells stained against the proliferation marker Ki67 (*red color*) and (**B**) apoptotic cells recognized by labeling DNA breaks induced by DNAse I (*red color*) in endometriotic implants obtained after killing the control, anti-VEGF, and pIC^{PEI} treated mice. Scale bar = 150 μm. (**C**) Cellular proliferation and (**D**) apoptosis among the three groups (mean + SEM). *P<.05 vs. control group.

García-Pascual. pIC^{PEI} inhibits endometriosis.. Fertil Steril 2015.

(35–38). Indeed, fluorescence faded progressively, even in control animals, to the point that nearly 60% had been lost in control vehicle-treated animals after 4 weeks.

To maximize the effects on neovessels, we began treatment with pIC^{PEI} the day after surgery to interfere with the revascularization taking place during the initial periods of engraftment (39). pIC^{PEI} moderately reduced the density of blood vessels, as shown by a noticeable, though not statistically significant, decrease in this parameter. It very likely did, however, interfere with the process of neovascularization in endometrial lesions, as shown by the fewer number of neovessels in pIC^{PEI}-treated animals compared with negative control. Provided that immature vessels are much more susceptible to pro/antiangiogenic effects than mature vessels (40), our results suggest that pIC^{PEI} is able to partially inhibit the growth of newly forming (immature) vessels, but not those of the mature type surrounded by α-SMA, which are less susceptible to antiangiogenic effects. This statement comes from the observation that pIC is able to interfere with sprouting angiogenesis of neovessels, as shown in aortic ring and tube formation assays in vitro (41). These findings are also in agreement with our recent findings (unpublished) that pIC^{PEI} is able to significantly decrease vessel density of tissues such as leiomyoma in which vascularization largely comprises immature α-SMA–free vessels (42). We speculate that the overall antiangiogenic effects of pIC^{PEI} were not dramatically evident in the grafts because vascularization of endometrial tissue comprises a mixture of both mature (α-SMA surrounded) and immature vessels (30, 32, 33). Because the effects of the VEGF blockade on overall neovascularization were more acute than those exerted by our compound, it is likely that pIC^{PEI} provides a less powerful antiangiogenic effect than traditional inhibition of VEGF.

The interplay between inhibition of angiogenesis and apoptosis in proliferating tissues is largely known (9, 10, 29, 43) despite not being understood at the molecular level.

Although restriction of nutrient supply owing to antiangiogenic events is known to lead to apoptosis of circumventing tissues (29), a reverse effect also has been reported, with induction of apoptosis in endothelial cells leading to antiangiogenic events (43). Interestingly, the effects of pIC^{PEI} on increased apoptosis were equal or of larger magnitude than those exerted by the VEGF inhibitor. Provided that antiangiogenic effects exerted by pIC^{PEI} were lower than those exerted by VEGF blockade we reason that a significant part of the proapoptotic effects exerted by pIC^{PEI} were not mediated by antiangiogenic dependent restriction of nutrient supply but instead through direct effects in endometriotic tissue. This speculation is supported by studies showing that pIC induces apoptosis in in vitro cultures of human endothelial (41) and tumor cells of malignant origin (24, 41). Further support comes from our recent finding that pIC^{PEI} induces moderate but clear apoptotic events even in primary in vitro cultures of benign tumors, such as leiomyomas (unpublished observations). It remains to be confirmed in further studies whether apoptosis induced by pIC^{PEI} in benign diseases, such as endometriosis and leiomyoma, is driven by the same molecular mechanism described in malignant tissues (16, 17, 24, 41).

Employment of Ad-mCherry for labeling, instead of GFP, prolonged the period during which noninvasive assessment could be reliably monitored (35–37). Extension of the time frame was sufficient to reveal a significant reduction in the implant size of anti-VEGF–treated animals versus control. In spite of its antiangiogenic and proapoptotic effects, administration of pIC^{PEI} did not, however, lead to significant reduction in implant size during the period of study. Owing to its lesser antiangiogenic profile versus CBO-P11, we speculate that a more prolonged treatment with pIC^{PEI} might have been necessary to reach the progressive collapse of the pathologic tissue and its subsequent reabsorption in such a way that shrinkage of tissue could be observed (12). However, further extension of the time of study is not possible, thus preventing us from testing this hypothesis in this mouse model. More specifically, the transient episomal expression of the Ad-virus required for labeling (44) and the presence of natural killer cells leading to xenograft rejection (45) do not allow further extension of the study time beyond 4–5 weeks in the nude mouse model. Our expectation that prolonged use of pIC^{PEI} might render more drastic effects over lesion size is based on our previous experience testing the effects of compounds with a similar moderate antiangiogenic profile, such as the dopamine agonist quinagolide. Indeed, when quinagolide was assayed over a short period of time (3 weeks) in our heterologous nude mouse model of endometriosis, only discrete effects on lesion size were reported (30). However when assayed over a prolonged period of time (4 months) in humans, this dopamine agonist was able to induce a dramatic shrinkage of endometriotic lesions (12). Besides the lack of sustained antiangiogenic effects over time, the lack of a complete immune system in this model might be an additional limitation for this drug to exert a more dramatic effect. Indeed, the antitumoral activity of pIC^{PEI} was originally ascribed to its capacity to boost the immune system in an interferon-dependent manner (13, 14). Given the role of the immune system in endometriosis (46, 47), the defective immunologic function in our nude model might have caused pIC^{PEI} to be unable to induce a more dramatic regression of the endometriotic lesion. To explore this possibility, we are currently investigating the effects of pIC^{PEI} on lesion size using a recently improved homologous mouse model of endometriosis (48) with an intact immune system.

CONCLUSION

We created a mouse model of endometriosis with the use of transgenic human endometrial tissue engineered to express the fluorescent protein mCherry to investigate the effects of treatment with pIC^{PEI}. We saw a decrease in neovascularization and an increased apoptosis rate in the transplanted endometriotic lesions treated with pIC^{PEI}, warranting further exploration of this treatment option. Longer time points are necessary to fully characterize the pIC^{PEI} profile; however, the results presented here suggest a plausible role for treatment with pIC^{PEI} in reducing lesion size.

REFERENCES

1. Galle PC. Clinical presentation and diagnosis of endometriosis. Obstet Gynecol Clin North Am 1989;16:29–42.
2. Sampson JA. Metastatic or embolic endometriosis due to the menstrual dissemination of endometrial tissue into the venous circulation. Am J Pathol 1927;3:93–110.43.
3. Giudice LC. Clinical practice. Endometriosis. N Engl J Med 2010;362:2389–98.
4. Rawson JM. Prevalence of endometriosis in asymptomatic women. J Reprod Med 1991;36:513–5.
5. Kupker W, Felberbaum RE, Krapp M, Schill T, Malik E, Diedrich K. Use of GnRH antagonists in the treatment of endometriosis. Reprod Biomed Online 2002;5:12–6.
6. Maas JW, Groothuis PG, Dunselman GA, de Goeij AF, Struijker-Boudier HA, Evers JL. Development of endometriosis-like lesions after transplantation of human endometrial fragments onto the chick embryo chorioallantoic membrane. Hum Reprod 2001;16:627–31.
7. Taylor RN, Lebovic DI, Mueller MD. Angiogenic factors in endometriosis. Ann N Y Acad Sci 2002;955:89–100.
8. Nap AW, Griffioen AW, Dunselman GA, Bouma–ter Steege JC, Thijssen VL, Evers JL, et al. Antiangiogenesis therapy for endometriosis. J Clin Endocrinol Metab 2004;89:1089–95.
9. Via LE, Gore-Langton RE, Pluda JM. Clinical trials referral resource. Current clinical trials administering the antiangiogenesis agent SU5416. Oncology (Williston Park) 2000;14:1312–23.
10. Kamba T, McDonald DM. Mechanisms of adverse effects of anti-VEGF therapy for cancer. Br J Cancer 2007;96:1788–95.
11. Feng D, Menger MD, Laschke MW. Vascular disrupting effects of combretastatin A4 phosphate on murine endometriotic lesions. Fertil Steril 2013;100:1459–67.
12. Gómez R, Abad A, Delgado F, Tamarit S, Simón C, Pellicer A. Effects of hyperprolactinemia treatment with the dopamine agonist quinagolide on endometriotic lesions in patients with endometriosis-associated hyperprolactinemia. Fertil Steril 2011;95:882–8.
13. Field AK, Tytell AA, Lampson GP, Hilleman MR. Inducers of interferon and host resistance. II. Multistranded synthetic polynucleotide complexes. Proc Natl Acad Sci U S A 1967;58:1004–10.
14. Levy HB, Law LW, Rabson AS. Inhibition of tumor growth by polyinosinic-polycytidylic acid. Proc Natl Acad Sci U S A 1969;62:357–61.
15. Fisher JC, Cooperband SR, Mannick JA. The effect of polyinosinic-polycytidylic acid on the immune response of mice to antigenically distinct tumors. Cancer Res 1972;32:889–92.

16. Kleinman ME, Yamada K, Takeda A, Chandrasekaran V, Nozaki M, Baffi JZ, et al. Sequence- and target-independent angiogenesis suppression by siRNA via TLR3. Nature 2008;452:591–7.
17. Bergé M, Bonnin P, Sulpice E, Vilar J, Allanic D, Silvestre JS, et al. Small interfering RNAs induce target-independent inhibition of tumor growth and vasculature remodeling in a mouse model of hepatocellular carcinoma. Am J Pathol 2010;177:3192–201.
18. Freeman AI, Al-Bussam N, O'Malley JA, Stutzman L, Bjornsson S, Carter WA. Pharmacologic effects of polyinosinic-polycytidylic acid in man. J Med Virol 1977;1:79–93.
19. Levine AS, Sivulich M, Wiernik PH, Levy HB. Initial clinical trials in cancer patients of polyriboinosinic-polyribocytidylic acid stabilized with poly-L-lysine, in carboxymethylcellulose [poly(ICLC)], a highly effective interferon inducer. Cancer Res 1979;39:1645–50.
20. Robinson RA, DeVita VT, Levy HB, Baron S, Hubbard SP, Levine AS. A phase I-II trial of multiple dose polyriboinosic-polyribocytidylic acid in pationts with leukemia or solid tumors. J Natl Cancer Inst 1976;57:599–602.
21. Pollack IF, Jakacki RI, Butterfield LH, Hamilton RL, Panigrahy A, Potter DM, et al. Antigen-specific immune responses and clinical outcome after vaccination with glioma-associated antigen peptides and polyinosinic-polycytidylic acid stabilized by lysine and carboxymethylcellulose in children with newly diagnosed malignant brainstem and nonbrainstem gliomas. J Clin Oncol 2014;32:2050–8.
22. Salazar AM, Erlich RB, Mark A, Bhardwaj N, Herberman RB. Therapeutic in situ autovaccination against solid cancers with intratumoral poly-ICLC: case report, hypothesis, and clinical trial. Cancer Immunol Res 2014;2:720–4.
23. Fujimura T, Nakagawa S, Ohtani T, Ito Y, Aiba S. Inhibitory effect of the polyinosinic-polycytidylic acid/cationic liposome on the progression of murine B16F10 melanoma. Eur J Immunol 2006;36:3371–80.
24. Tormo D, Checinska A, Alonso-Curbelo D, Perez-Guijarro E, Canon E, Riveiro-Falkenbach E, et al. Targeted activation of innate immunity for therapeutic induction of autophagy and apoptosis in melanoma cells. Cancer Cell 2009;16:103–14.
25. Alonso-Curbelo D, Soengas MS. Self-killing of melanoma cells by cytosolic delivery of dsRNA: wiring innate immunity for a coordinated mobilization of endosomes, autophagosomes and the apoptotic machinery in tumor cells. Autophagy 2010;6:148–50.
26. Pollacco J, Sacco K, Portelli M, Schembri-Wismayer P, Calleja-Agius J. Molecular links between endometriosis and cancer. Gynecol Endocrinol 2012;28:577–81.
27. Okada S, Ishii K, Yamane J, Iwanami A, Ikegami T, Katoh H, et al. In vivo imaging of engrafted neural stem cells: its application in evaluating the optimal timing of transplantation for spinal cord injury. FASEB J 2005;19:1839–41.
28. Masuda H, Maruyama T, Hiratsu E, Yamane J, Iwanami A, Nagashima T, et al. Noninvasive and real-time assessment of reconstructed functional human endometrium in NOD/SCID/gamma c(null) immunodeficient mice. Proc Natl Acad Sci U S A 2007;104:1925–30.
29. Garcia-Pascual CM, Zimmermann RC, Ferrero H, Shawber CJ, Kitajewski J, Simon C, et al. Delta-like ligand 4 regulates vascular endothelial growth factor receptor 2–driven luteal angiogenesis through induction of a tip/stalk phenotype in proliferating endothelial cells. Fertil Steril 2013;100:1768–76.
30. Delgado-Rosas F, Gomez R, Ferrero H, Gaytan F, Garcia-Velasco J, Simon C, et al. The effects of ergot and non–ergot-derived dopamine agonists in an experimental mouse model of endometriosis. Reproduction 2011;142:745–55.
31. Olive DL, Lindheim SR, Pritts EA. New medical treatments for endometriosis. Best Pract Res Clin Obstet Gynaecol 2004;18:319–28.
32. Hull ML, Charnock-Jones DS, Chan CL, Bruner-Tran KL, Osteen KG, Tom BD, et al. Antiangiogenic agents are effective inhibitors of endometriosis. J Clin Endocrinol Metab 2003;88:2889–99.
33. Dabrosin C, Gyorffy S, Margetts P, Ross C, Gauldie J. Therapeutic effect of angiostatin gene transfer in a murine model of endometriosis. Am J Pathol 2002;161:909–18.
34. Stone RL, Sood AK, Coleman RL. Collateral damage: toxic effects of targeted antiangiogenic therapies in ovarian cancer. Lancet Oncol 2010;11:465–75.
35. Fortin M, Lepine M, Page M, Osteen K, Massie B, Hugo P, et al. An improved mouse model for endometriosis allows noninvasive assessment of lesion implantation and development. Fertil Steril 2003;80(Suppl 2):832–8.
36. Fortin M, Lepine M, Merlen Y, Thibeault I, Rancourt C, Gosselin D, et al. Quantitative assessment of human endometriotic tissue maintenance and regression in a noninvasive mouse model of endometriosis. Mol Ther 2004;9:540–7.
37. Liu B, Wang NN, Wang ZL, Hong SS, Li JT, Ding HJ, et al. Improved nude mouse models for green fluorescence human endometriosis. J Obstet Gynaecol Res 2010;36:1214–21.
38. Wang N, Hong S, Tan J, Ke P, Liang L, Fei H, et al. A red fluorescent nude mouse model of human endometriosis: advantages of a non-invasive imaging method. Eur J Obstet Gynecol Reprod Biol 2014;176:25–30.
39. Eggermont J, Donnez J, Casanas-Roux F, Scholtes H, Van Langendonckt A. Time course of pelvic endometriotic lesion revascularization in a nude mouse model. Fertil Steril 2005;84:492–9.
40. Benjamin LE, Golijanin D, Itin A, Pode D, Keshet E. Selective ablation of immature blood vessels in established human tumors follows vascular endothelial growth factor withdrawal. J Clin Invest 1999;103:159–65.
41. Guo Z, Chen L, Zhu Y, Zhang Y, He S, Qin J, et al. Double-stranded RNA–induced TLR3 activation inhibits angiogenesis and triggers apoptosis of human hepatocellular carcinoma cells. Oncol Rep 2012;27:396–402.
42. Aitken E, Khaund A, Hamid SA, Millan D, Campbell S. The normal human myometrium has a vascular spatial gradient absent in small fibroids. Hum Reprod 2006;21:2669–78.
43. Pauli SA, Tang H, Wang J, Bohlen P, Posser R, Hartman T, et al. The vascular endothelial growth factor (VEGF)/VEGF receptor 2 pathway is critical for blood vessel survival in corpora lutea of pregnancy in the rodent. Endocrinology 2005;146:1301–11.
44. Suo G, Sadarangani A, Lamarca B, Cowan B, Wang JY. Murine xenograft model for human uterine fibroids: an in vivo imaging approach. Reprod Sci 2009;16:827–42.
45. Kawahara T, Douglas DN, Lewis J, Lund G, Addison W, Tyrrell DL, et al. Critical role of natural killer cells in the rejection of human hepatocytes after xenotransplantation into immunodeficient mice. Transpl Int 2010;23:934–43.
46. Herington JL, Bruner-Tran KL, Lucas JA, Osteen KG. Immune interactions in endometriosis. Expert Rev Clin Immunol 2011;7:611–26.
47. Berkkanoglu M, Arici A. Immunology and endometriosis. Am J Reprod Immunol 2003;50:48–59.
48. Cheng CW, Licence D, Cook E, Luo F, Arends MJ, Smith SK, et al. Activation of mutated K-ras in donor endometrial epithelium and stroma promotes lesion growth in an intact immunocompetent murine model of endometriosis. J Pathol 2011;224:261–9.